Antidiabetic Potential and Chemical Profiling of Chloroform Fraction from *Euclea racemosa subsp. schimperi In Vitro*

Hanan M. El-Tantawy [1*]

Abstract

Background: The chloroform fraction ($CHCl_3$ Fr.) of *Euclea racemosa subsp. schimperi* has enormous interest for its potential therapeutic properties in managing diabetes and oxidative stress-related conditions. This study aimed to evaluate the chemical composition and biological activities of $CHCl_3$ Fr. through LC-ESI-MS/MS and GC-MS analyses. Methods: The $CHCl_3$ Fr. was analyzed using LC-ESI-MS/MS for identification of bioactive compounds, and its inhibitory effects on α-amylase and α-glucosidase were assessed in vitro. Additionally, the impact on insulin secretion, C-peptide levels, and oxidative stress markers (MDA and NO) were measured. Results: Nineteen bioactive compounds, including flavonoids, pentacyclic triterpenes, and monounsaturated fatty acids, were identified in the chloroform fraction ($CHCl_3$ Fr.). It significantly inhibited α-amylase and α-glucosidase, with IC_{50} values of 21.16 ± 2.13 and 13.49 ± 0.83 µg/ml, respectively. In insulin-resistant Huh7 cells, $CHCl_3$ Fr. reduced glucose levels and increased insulin and C-peptide levels ($p < 0.05$). While it decreased malondialdehyde and nitric oxide, it did not significantly enhance catalase or total antioxidant capacity ($p > 0.05$). Compared to metformin, $CHCl_3$ Fr. showed less efficacy but may improve insulin resistance and reduce oxidative stress, likely due to its bioactive compounds. Conclusion: The presence of diverse bioactive compounds contributes to the antidiabetic effects of $CHCl_3$ Fr. from E. r. ssp. shimperi, showed its potential as a natural therapeutic agent for diabetes management and oxidative stress reduction. Further investigations are warranted to explore its clinical applications and underlying mechanisms.

Keywords: E. r. ssp. schimperi, bioactive compounds, insulin resistance, α-amylase, oxidative stress

Significance | This study determines the potential therapeutic benefits of *E. r. ssp. schimperi* in managing insulin resistance and oxidative stress.

*Correspondence. Hanan M. El-Tantawy, Medicinal and Aromatic Plants Department, Desert Research Center, Cairo, Egypt.
E-mail: hanantantawy143@gmail.com.

Editor Md Shamsuddin Sultan Khan And accepted by the Editorial Board October 10, 2024 (received for review August 12, 2024)

Introduction

Insulin resistance arises from either inadequate insulin secretion or a diminished capacity of insulin to facilitate glucose absorption, leading to postprandial hyperglycemia, and disturbances in protein, lipid, and carbohydrate metabolism, as well as cellular oxidative stress (Telagari & Hullatti, 2015). Oxidative stress results when reactive species overwhelm antioxidant defenses, causing cellular damage (Mishra & Mishra, 2017). This process notably impacts the heart and peripheral vascular systems (Steiner et al., 1967). Oxidative stress markers such as malondialdehyde (MDA) and nitric oxide (NO) increase due to protein, lipid, and DNA oxidation (Gaweł et al., 2004; Yang et al., 2011). Antioxidant markers include catalase (CAT), which catalyzes the conversion of hydrogen peroxide into water and oxygen, and total antioxidant capacity (TAC), a non-enzymatic marker that reflects overall antioxidant status (Tamil et al., 2010; Torun et al., 2009).

Insulin resistance manifests in reduced responsiveness of the responsiveness of the liver, muscles, and adipose tissue to insulin's

Author Affiliation.
[1] Medicinal and Aromatic Plants Department, Desert Research Center, Cairo, Egypt.

Please Cite This:
Hanan M. El-Tantawy (2024). "Antidiabetic Potential and Chemical Profiling of Chloroform Fraction from Euclea racemosa subsp. schimperi In Vitro", Journal of Angiotherapy, 8(10),1-13. 9977.

physiological functions (Ormazabal et al., 2018). The in vitro Huh7-IR cell model is widely used for pharmacological and metabolic research focused on hepatic insulin resistance. This model is created by inducing insulin resistance in the Huh7 cell line through high-glucose exposure, followed by treatment with metformin to counteract the effects of excessive insulin. The Huh7 cell line, derived from well-differentiated hepatocellular carcinoma, closely mimics primary human hepatocytes (Villalva-Pérez et al., 2020). Insulin, a natural hormone produced by pancreatic islets, aids cellular glucose utilization for energy (Steiner et al., 1967; Villalva-Pérez et al., 2020).

C-peptide, released from pancreatic beta cells during insulin cleavage from proinsulin, remains in the bloodstream longer than insulin, providing a more reliable indicator of insulin secretion in liver disease (Rigler et al., 1999; Leighton et al., 2017). Acarbose, a pharmaceutical inhibitor of α-glucosidase and α-amylase, helps regulate postprandial blood glucose and can reduce diabetes-related complications (Mechchate et al., 2021). Metformin, a standard therapy, effectively reduces insulin resistance and associated biomarkers in the IR-Huh7 model (Villalva-Pérez et al., 2020). Although insulin and oral hypoglycemic agents help manage hyperglycemia and lower diabetes risk, they are often accompanied by side effects (Gong et al., 2020). As a result, identifying safe, plant-based antidiabetic agents has gained attention due to their lower cost and fewer adverse effects (Grover et al., 2002).

Plants in the Euclea genus (family Ebenaceae) possess antidiabetic, anticancer, and antioxidant properties (Botha, 2016). *Euclea racemosa subsp. schimperi* (E. r. ssp. schimperi) is rich in bioactive secondary metabolites, including anthraquinones, pentacyclic triterpenes, saponins, fatty acids, phenolic acids, coumarins, and flavonoids (Mekonnen et al., 2018). Traditionally, it is used in Kenyan medicine to manage diabetes mellitus and in other treatments, such as for cancer, toothaches, diarrhea, malaria, and skin irritations (Odukoya et al., 2022; Taye et al., 2023). This plant exhibits significant antioxidant activity, attributed to its high levels of flavonoids like quercetin, myricitrin, myricetin-3-O-arabinopyranoside, and rutin (Asres et al., 2006). Furthermore, methyljuglone isolated from this plant has been shown to inhibit the formation of 12(S)-HETE, an inflammatory mediator (Wube et al., 2005).

This study evaluates the inhibitory effects of the methanolic extract and fractions of E. r. ssp. schimperi on α-glucosidase and α-amylase enzymes. The most effective fraction is then applied to an insulin-resistant human cell model (IR-Huh7) to measure levels of insulin, glucose, C-peptide, oxidative biomarkers (MDA and NO), and antioxidant indicators (CAT and TAC). This fraction is further analyzed using GC-MS and LC-MS/MS for compound identification.

2. Materials and Methods

2.1. Plant Material

The aerial parts of *Euclea racemosa subsp. schimperi* (A.DC.) F. White, family Ebenaceae, were collected from the Elba mountain region. Dr. Mahmoud Ali, Associate Professor of Plant Ecology at the Desert Research Centre herbarium, confirmed the plant's identification, assigning it a voucher number (CAIH-1254-R).

2.2. Extraction and Fractionation

After collection, the aerial parts of *E. racemosa* subsp. *schimperi* were washed with distilled water, air-dried, and finely ground. Using the maceration technique, 1.5 kg of powdered plant material was extracted with 80% ethanol (4.5 L per extraction) every 48 hours at room temperature. The collected extracts were concentrated under reduced pressure at 45°C until dry, yielding 67.32 g of dried extract. Initial biological screening assessed the crude extract's potential as an α-glucosidase and α-amylase inhibitor. The entire extract was then fractionated through bio-guided liquid-liquid partitioning in a separating funnel. The extract was suspended in 600 ml of 70% aqueous methanol and partitioned using n-hexane, chloroform, ethyl acetate, butanol, and water to obtain fractions: n-hexane (Hex. Fr., 12 g), chloroform (CHCl3 Fr., 11.29 g), ethyl acetate (EtOAc Fr., 8.93 g), butanol (BtOH Fr., 15.52 g), and aqueous (aqueous Fr., 19.30 g). The most bioactive fraction was subsequently evaluated in vitro on the insulin-resistant Huh7 cell model. Phytoconstituents in this fraction were identified using GC-MS and LC-ESI-MS techniques.

2.3. Enzymatic Inhibition Assays In Vitro

2.3.1. α-Amylase Inhibition Assay

The α-amylase inhibitory activity was tested with a diluted plant extract in 1% dimethyl sulfoxide (DMSO) at various concentrations (0.25 to 500 µg/ml). The α-amylase inhibitory activity was evaluated following the protocol of the α-amylase Inhibitor Screening Kit 95035 (USA) as described by Telagari et al. (2015).

2.3.2. α-Glucosidase Inhibition Assay

The α-glucosidase inhibitory activity was measured for extracts dissolved in DMSO across concentrations ranging from 0.25 to 500 µg/ml in phosphate buffer. The assay followed the α-glucosidase Inhibitor Screening Kit protocol (Catalog # K938-100; 100 assays) according to Shai et al. (2011).

2.4. Cell Line Preparation

The Huh7 cell line, a well-differentiated hepatocellular carcinoma-derived line, was sourced from Nawah Scientific in Cairo, Egypt, in a 25-ml T-culture flask. All reagents were from Gibco, Thermo Fisher Scientific, Germany. After removing the culture medium, the cells were washed three times with Dulbecco's phosphate-buffered saline (PBS; NaCl 0.138 M, KCl 0.003 M, pH 7.4). The Huh7 cells were subcultured in Dulbecco's Modified Eagle Medium (DMEM) supplemented with 10% fetal bovine serum (FBS), 1% antibiotic/antimycotic solution, high glucose (4.5 g/l), L-glutamine,

sodium pyruvate, and PSA [1% penicillin G sodium (10,000 IU), streptomycin (10 mg), and amphotericin B (25 µg)]. Cells were incubated at 37°C in a 5% CO_2 atmosphere and monitored until they reached 70% confluence. The cells were then harvested using 0.25% trypsin-EDTA. Cells from the third and fourth passages, which exhibited optimal viability, were used in subsequent experiments (Woźniak & Paduch, 2012).

2.4.1. Induction of an Insulin-Resistant (IR) Model

Insulin resistance in Huh7 cells was induced following the protocol by Jakovljevic et al. (2021). Cells were treated with human insulin (Catalog No. 11061-68-0, Sigma-Aldrich, USA) at a concentration of 60 nM (10 mU/ml) for 24 hours to develop IR through chronic exposure. Non-IR Huh7 control cells were cultured in medium without fetal bovine serum (FBS) for 24 hours. Following treatment, the cells were stabilized in supplemented medium after washing three times with PBS. Insulin resistance was confirmed by measuring glucose and insulin levels, as described by Villalva-Pérez et al. (2020).

2.4.2. Preparation of $CHCl_3$ Fraction for Treatment

To assess the effect of the $CHCl_3$ fraction on cells, 0.1 g of semisolid $CHCl_3$ fraction was dissolved in 1% dimethyl sulfoxide (DMSO), sonicated briefly (5 seconds), aliquoted, and stored at -20°C as a stock solution. A working solution was prepared by diluting the stock with 1% DMSO to achieve concentrations ranging from 0.001 to 100 µg/ml for EC_{50} determination. Metformin (purity ≥97.9%, Sigma-Aldrich, St. Louis, MO, USA, CAS#: 657-24-9) was prepared similarly.

2.4.3. EC_{50} Determination for $CHCl_3$ Fraction

The cell proliferation effect of the $CHCl_3$ fraction was measured using the Vybrant® MTT Cell Proliferation Assay Kit (Catalog No. M6494, Thermo Fisher, Germany) following Liu et al. (1997). This colorimetric assay is based on the reduction of yellow MTT to purple formazan crystals. All treatments were conducted in triplicates.

2.5. Effect of $CHCl_3$ Fraction on Huh7 Cells

After inducing insulin resistance, cells were washed three times with PBS, followed by supplementation with fresh media. Cells were seeded at 5×10^5 cells/well in 96-well plates, treated with $CHCl_3$ fraction and metformin at their respective EC_{50} doses for 48 hours, washed with PBS, and cultured in medium without FBS. Various assays were conducted to evaluate the effects on insulin sensitivity and glucose metabolism.

2.5.1. Glucose Levels

Glucose levels in IR-Huh7 cells were measured using an endpoint colorimetric assay with the glucose kit (Catalog No. SU019, Reactivos GPL, Barcelona, Spain), which measures glucose oxidation to gluconic acid catalyzed by glucose oxidase.

2.5.2. Insulin Levels

The insulin levels in treated cells were determined using a human insulin ELISA assay (Catalog No. E-EL-H2665, Elabscience Biotechnology, USA) following the sandwich-ELISA principle.

2.5.3. C-Peptide Levels

C-peptide levels were measured using the human C-Peptide ELISA Kit (Catalog No. EH-0387, Fine Test, Wuhan, China) via enzyme-linked immunosorbent assay (ELISA).

2.6. Oxidative Biomarkers: MDA and NO

2.6.1. MDA Assay

Malondialdehyde (MDA) levels were assessed using the thiobarbituric acid reactive substances (TBARS) method according to Draper and Hadley (1990), with the MDA colorimetric assay kit (Catalog No. E-BC-K025-S, Elabscience Biotechnology, USA).

2.6.2. NO Assay

Nitric oxide (NO) levels were quantified by measuring nitrite in the culture medium, as an indicator of NO production, using the Nitric Oxide colorimetric assay kit (Catalog No. E-BC-K035-M, Elabscience Biotechnology, USA).

2.7. Antioxidative Biomarkers: CAT and TAC

2.7.1. TAC Levels

Total antioxidant capacity (TAC) was measured using the TAC colorimetric assay kit (Catalog No. E-BC-K136-M, Elabscience Biotechnology, USA) following the method described by Prieto et al. (1999), with absorbance measured at 695 nm.

2.7.2. CAT Levels

Catalase (CAT) activity was measured using the CAT Activity Colorimetric Kit (Catalog No. EBC-K031-S, Elabscience Biotechnology, USA). The assay detects the formation of a yellow complex measured at 405 nm.

2.8. GC-MS Analysis of the $CHCl_3$ Fraction

The chloroform fraction from aerial parts of *E. racemosa* subsp. *schimperi* was analyzed by gas chromatography-mass spectrometry (GC-MS) using a Thermo Scientific Trace GC-ISQ mass spectrometer with a direct capillary column (TG-5MS, 30 m × 0.25 µm, 0.25 µm film thickness). The column oven temperature was initially set at 50°C, increased by 5°C/min to 250°C, and then to 300°C at 30°C/min, holding for 2 minutes. Helium was used as the carrier gas at a flow rate of 1 mL/min. The injector and MS transfer line temperatures were maintained at 270°C and 260°C, respectively. The diluted sample was injected in split mode, using an AS1300 auto-sampler. Mass spectra were obtained in full scan mode (50–650 m/z) with 70 eV ionization voltage, and components were identified by comparing spectra with the NIST 14 and WILEY 09 databases (Abd El-Kareem et al., 2016).

2.9. LC-ESI-MS Analysis of the $CHCl_3$ Fraction

The $CHCl_3$ fraction from *E. racemosa* subsp. *schimperi* was analyzed using liquid chromatography-electrospray ionization-tandem mass spectrometry (LC-ESI-MS/MS) on an Exion LCAC

system with a SCIEX Triple Quad 5500+ MS/MS detector and an Ascentis® Express C18 column (2.1 × 150 mm, 2.7 µm). The mobile phases were 5 mM ammonium formate (pH 3) and acetonitrile, with the following gradient: 5% B at 0–1 min, 5–100% B at 1–20 min, 100% B at 20–25 min, and 5% B at 25.01–30 min. Flow rate was 0.3 ml/min, with injection volume set to 5 µL. The source temperature was 500°C, with gas pressures of 45 psi for ion sources 1 and 2, 25 psi curtain gas, and ion spray voltages of -4500 V (negative mode) and 5500 V (positive mode). The collision energies were set at -35 and 35 for negative and positive ionization modes, respectively. MS-DIAL software was used to identify compounds (Hassan, 2022).

2.10 Statistical Analysis

Data were analyzed using GraphPad Prism 8.4.2 (San Diego, USA). Results are presented as means ± standard deviation (SD) for parametric data. Statistical significance was determined using ANOVA, followed by post hoc tests for comparisons between multiple groups. Significance was set at $p \leq 0.05$, with $p < 0.01$ indicating high significance.

3. Results

The ethanol extract (80%) from *E. racemosa* subsp. *schimperi* aerial parts was fractionated via chromatography into five distinct fractions: hexane (Hex Fr.), chloroform ($CHCl_3$ Fr.), ethyl acetate (EtOAc Fr.), butanol (BtOH Fr.), and aqueous (Aqueous Fr.). Each fraction was subsequently tested for its inhibitory effects on α-amylase and α-glucosidase enzymes, revealing that the $CHCl_3$ fraction exhibited the most potent inhibitory action in vitro. Consequently, $CHCl_3$ Fr. was selected for further evaluation of its effects on insulin resistance in diabetes (IRD) using Huh7-IR cells. Chemical profiling of this fraction was carried out via GC-MS and LC-ESI-MS.

3.1. Inhibition of α-amylase and α-glucosidase by $CHCl_3$ Fraction

Inhibiting α-glucosidase and α-amylase enzymes is beneficial in controlling blood glucose levels in type 2 diabetes, as it helps reduce the postprandial rise in glucose (Tundis et al., 2010). The crude 70% ethanolic extract of *E. racemosa* displayed moderate inhibitory effects on α-amylase and α-glucosidase with IC_{50} values of 99.78 ± 4.92 and 85.73 ± 3.64 µg/ml, respectively. Guided by bioactivity, fractionation produced five distinct fractions, each tested for enzyme inhibition potential, yielding significant results for $CHCl_3$ Fr., which had IC_{50} values of 21.16 ± 2.13 µg/ml and 13.49 ± 0.83 µg/ml for α-amylase and α-glucosidase inhibition, respectively. However, the IC_{50} values were slightly higher than the standard drug acarbose, which showed IC_{50} values of 12.30 ± 0.89 µg/ml for α-amylase and 3.13 ± 0.43 µg/ml for α-glucosidase (Table 1).

These findings underscore the significant inhibitory potential of $CHCl_3$ Fr. on α-amylase and α-glucosidase. Although it was slightly less effective than acarbose, it nonetheless demonstrates a potent antidiabetic activity. This result prompted further evaluation of $CHCl_3$ Fr.'s antidiabetic effects on Huh7-IR cells by measuring various diabetes markers, including glucose, insulin, and C-peptide levels, as well as antioxidant markers (CAT and TAC) and oxidative stress markers (MDA and NO).

3.2. Viability of IR-Huh7 Cells Treated with Metformin and $CHCl_3$ Fraction

To assess cell viability and the impact of $CHCl_3$ Fr. and metformin on IR-Huh7 cells, treatments were applied at various concentrations (0.001 to 100 µg/ml) over a 48-hour period. Cell viability in IR-Huh7 cells was observed to be favorable at the EC_{50} concentrations of $CHCl_3$ Fr. (4.89 ± 2.25 µg/ml) and metformin (0.022 ± 0.003 µg/ml), which were selected as the effective treatment doses for IR-Huh7 cells (Figure 1). This viability analysis highlights the promising therapeutic effect of $CHCl_3$ Fr. at appropriate dosages.

These results lay a foundation for further exploring $CHCl_3$ Fr. as a potential antidiabetic agent, particularly given its notable enzyme inhibitory activity and the favorable cellular response in insulin-resistant models.

3.3. Glucose, Insulin, and C-peptide Levels in Huh7-IR Cells Compared with NC Group

To assess the impact of $CHCl_3$ Fr. on Huh7-IR cells over 48 hours, cells were treated with 4.89 ± 0.25 µg/ml of $CHCl_3$ Fr. and compared to untreated cells (negative control, NC) as well as to cells treated with 0.022 ± 0.003 µg/ml metformin (positive control).

3.3.1. Glucose Levels

Treatment with $CHCl_3$ Fr. significantly reduced glucose levels in Huh7-IR cells compared to untreated cells ($p < 0.05$), as shown in Figure 2a. Metformin treatment resulted in a more pronounced decrease in glucose levels compared to both untreated cells ($p < 0.001$) and $CHCl_3$ Fr. treated cells ($p < 0.05$), underscoring its stronger glucose-lowering effect (Figure 2a).

3.3.2. Insulin Levels

Increased insulin levels were observed in both $CHCl_3$ Fr. and metformin-treated groups, indicating improved glucose regulation. Insulin levels were significantly higher than in the control group, with p-values of <0.05 for $CHCl_3$ Fr. and <0.0001 for metformin. Moreover, metformin demonstrated a statistically significant advantage over $CHCl_3$ Fr. ($p < 0.0001$), suggesting enhanced insulin production potential (Figure 2b).

3.3.3. C-peptide Levels

Consistent with the insulin findings, C-peptide levels significantly improved in $CHCl_3$ Fr. and metformin groups compared to untreated cells ($p < 0.05$ and $p < 0.0001$, respectively). This suggests that both $CHCl_3$ Fr. and metformin enhance insulin secretion and facilitate glucose uptake in Huh7-IR cells, reducing insulin resistance (Figure 2c). These results collectively indicate that $CHCl_3$

Fr. mitigates insulin resistance in Huh7-IR cells, though metformin remains more effective.

3.4. Levels of MDA and NO in IR-Huh7 Cells

MDA and NO levels were significantly reduced in the $CHCl_3$ Fr. group compared to the NC group ($p < 0.05$), as shown in Figures 3a and 3b. Additionally, a significant difference was observed between $CHCl_3$ Fr. and metformin groups ($p = 0.0001$), indicating the potential of $CHCl_3$ Fr. to attenuate oxidative stress in IR-Huh7 cells, albeit less effectively than metformin.

3.5. Levels of CAT and TAC in IR-Huh7 Cells

No significant changes in CAT and TAC levels were observed in cells treated with $CHCl_3$ Fr. compared to untreated cells ($p > 0.05$). However, metformin treatment significantly elevated CAT and TAC levels relative to the control group ($p < 0.001$), highlighting metformin's notable antioxidant capacity (Figures 3c and 3d).

3.6. GC-MS Analysis of $CHCl_3$ Fraction of E. r. ssp. schimperi

The $CHCl_3$ Fr. composition of *E. racemosa* subsp. *schimperi* was analyzed using GC-MS, yielding 25 tentatively identified compounds eluted between 20.09 and 41.78 minutes (Figure 4). Identification was based on comparisons with the NIST, NBS, and Wiley libraries. Table 2 lists the major bioactive compounds, including 14 fatty compounds (71.97%), mainly unsaturated fatty acids (45.1%). Notable compounds include 9-octadecenoic acid (Z) (25.69%), cis-vaccenic acid (12.13%), erucic acid (5.32%), and cis-11-eicosenoic acid (1.96%). The composition also included fatty acid esters (24.04%) and small proportions of saturated fatty acids, glycerides, triterpenes, and sesquiterpenes, with 9-octadecenoic acid (oleic acid) as the most abundant constituent.

These findings provide insights into the bioactive potential of $CHCl_3$ Fr. for antidiabetic therapy, supported by its chemical profile rich in fatty acids and other functional bioactive compounds.

3.7. LC-ESI-MS Analysis of $CHCl_3$ Fraction of E. r. ssp. schimperi

The chemical profile of the $CHCl_3$ fraction from *E. r. ssp. schimperi* was investigated using LC-ESI-MS/MS for comprehensive identification of compounds. The analysis utilized both positive (+ve) and negative (-ve) ionization modes, examining retention times (Rt), molecular ions, and MS/MS fragment ions to elucidate compound structures. Literature data were then cross-referenced to confirm tentative identifications. Nineteen compounds, representing classes such as flavonoids, phenolic acids, and triterpenes, were identified based on LC-ESI-MS chromatograms in both ionization modes (Figure 5, Table 3). Among them were notable flavonoids including kaempferol, myricetin, and quercetin, as well as triterpenes in aglycone or glycosylated forms. Glycoside groups were identified through the neutral losses of hexoside and deoxyhexose at m/z 162 and 146, respectively (Spínola et al., 2015).

3.8. Flavonoid Compounds:

Compound 1 was identified in both ionization modes, with molecular ions at m/z 465 (M+H)+ and 463 (M-H)-, showing fragmentation at m/z 319 [(M+H)-146]+ and 316.9 [(M-H)-146]-, corresponding to deoxyhexose loss. Fragmentation patterns suggest myricetin aglycone with peaks at m/z 319 (+ve) and 317 (-ve), consistent with myricetin-O-deoxyhexoside, possibly myricitrin (Nguyen et al., 2013; Abu-Reidah et al., 2015).

Compound 2 exhibited ions at m/z 447 (M-H)- and 449 (M+H)+, with characteristic fragment peaks at m/z 301 [(M-H)-146]- and 303 [(M+H)-146]+. This fragmentation pattern, alongside ions at m/z 179, 151, and 121, is consistent with quercetin-O-deoxyhexoside, likely quercitrin (Pereira et al., 2017; Chaudharya et al., 2011; Abu-Reidah et al., 2015).

Compound 3, kaempferol-O-rhamnoside, was tentatively identified based on the peak at m/z 431 (M-H)- and 433 (M+H)+, with major fragments at m/z 285.0 and 286.9, indicating deoxyhexose loss and the presence of kaempferol aglycone (Li et al., 2016; Chaudharya et al., 2011).

Compounds 6 and 7 were detected at m/z 287 (M-H)- and 271 (M-H)-. The former is attributed to eriodictyol aglycone based on fragments at m/z 135 and 151, while the latter is identified as naringenin with fragment peaks at m/z 177, 151, and 119 (Vijayan et al., 2019; Goufo et al., 2020).

Compound 8 at m/z 331 (M+H)+ is identified as tricin with characteristic fragmentation patterns at m/z 315 [(M+H)-CH3]+ and 300 [(M+H)-2CH3]+, confirming its flavone structure (Li et al., 2016).

Compound 9 was identified as dihydroxy dimethoxy flavone with an [M-H]- ion at m/z 313, fragmenting to m/z 283, indicative of methoxy loss. This result aligns with previous reports on flavonoid composition (Attia et al., 2022).

The compounds identified in the $CHCl_3$ fraction of *E. r. ssp. schimperi* exhibit significant structural diversity and bioactive potential, supporting their potential therapeutic effects in metabolic and antioxidant applications. The major flavonoid compounds, including myricetin, quercetin, and kaempferol derivatives, are shown in Table 3 and Figure 5, providing a detailed characterization of the chemical profile in this fraction.

Other Compounds

Compound 10: The molecular ion $[M+H]^+$ was detected at m/z 181, with a fragmentation pattern showing m/z 163 [(M+H)-H_2O]+, 135 [(M+H)-H_2O-CO]+, and 89. This pattern tentatively identified the compound as caffeic acid, aligning with previous findings (Avula et al., 2020; El-Tantawy et al., 2022).

Compound 12: Identified as hexahydroxydiphenoyl (HHDP) galloylglucose, this compound showed [M-H]- at m/z 633, with MS^2 data revealing a fragment at m/z 481 [(M-H)-152] indicating loss of a galloyl moiety and a further fragment at m/z 301 [(M-H)-332]- corresponding to the HHDP unit (El-Sayed et al., 2021).

Compound 4: Detected at m/z 202.2 [M+H]+, this compound had fragments at m/z 172 [(M+H)-OCH_3]+, 144 [(M+H)-OCH_3-CO]+,

Table 1. IC_{50} values of different fractions of *Euclea racemosa* subsp *schimperi* against α-amylase and α-glycosidase

Fractions/ acarbose	IC_{50} µg/ml	
	α-amylase	α-glycosidase
Crude ethanolic 70%	99.78±4.92	85.73 ±3.64
Hex. Fr.	58.59 ±3.96	49.17±1.79
$CHCl_3$ Fr.	21.16 ± 2.13	13.49± 0.83
EtOAc Fr.	182.66 ± 8.21	122.10± 4.19
BtOH Fr.	130.75±6.23	103.51±3.94
Aqueous Fr.	163.68± 7.95	90.62± 3.87
Acarbose (drug)	12.30±0.89	3.13±0.43

IC50 valueIs is the half-maximal inhibitory concentration, IC50 calculated as ± SD (n = 3).

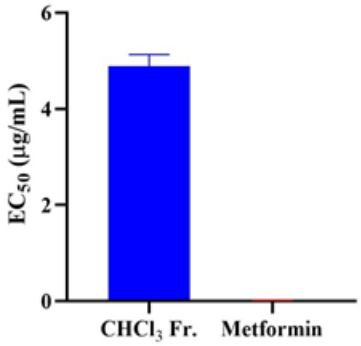

Figure 1. EC_{50} of $CHCl_3$ and Metformin in IR-Hub cells was a half maximum effective concentration.

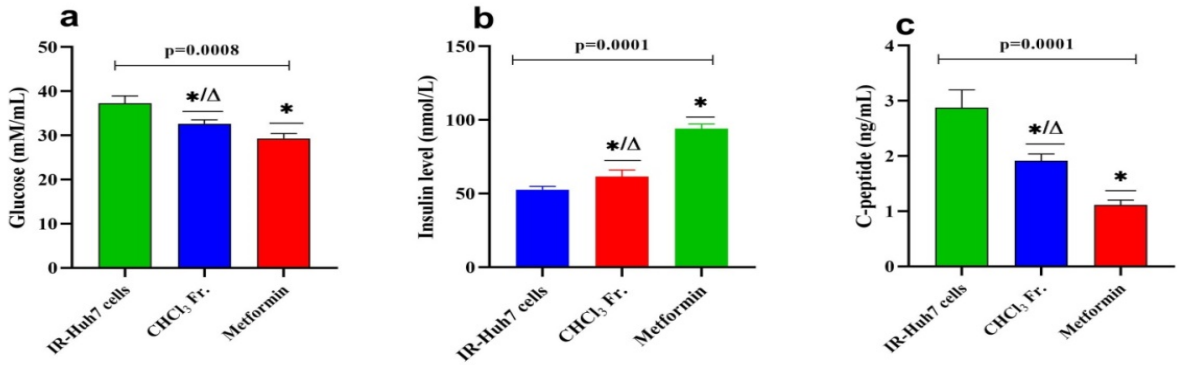

Figure 2. The effect of $CHCl_3$ Fr. in IR-Huh7 cells on (a) glucose level in culture media, (b) insulin level, and (c) C-peptide level.

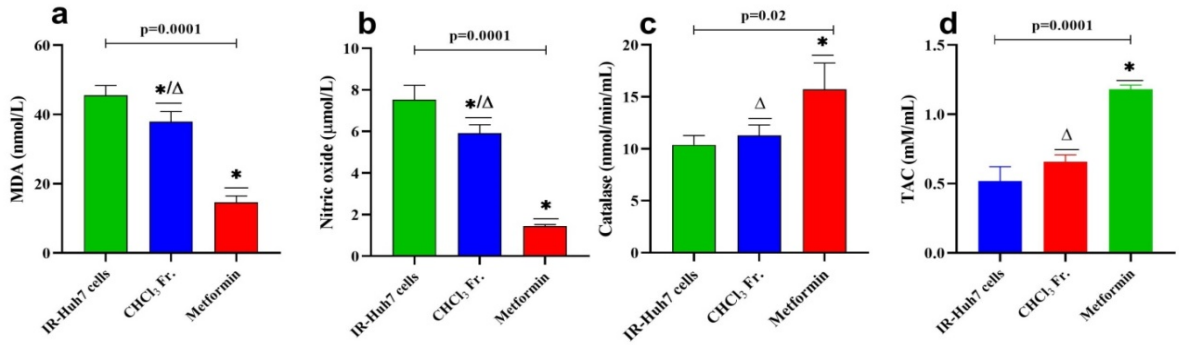

Figure 3. (a) Malonaldehyde level and (b) Nitric oxide level. (c) Catalase activity, and (d) Total antioxidant capacity in IR-Huh7 cells by $CHCl_3$. All data are presented as mean and standard deviation. *: statistical significance compared to the IR-Huh7 cells (NC), #: statistical significance compared to the $CHCl_3$ Fr. Δ: statistical significance compared to the Metformin (PC).

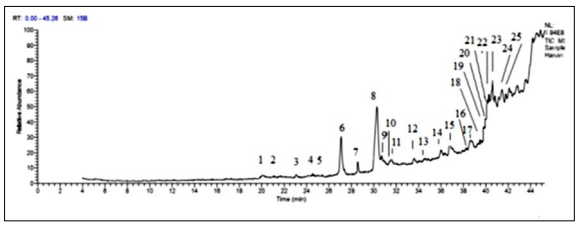

Figure 4. GC-mass analysis of $CHCl_3$ from of *E.r.* ssp. *schimperi* aerial parts.

Table 2. Phyto-components identified in the non-polar extract of *E.r* ssp. *schimperi* aerial parts by GC-MS:

NO.	RT	Peak of area%	M`WT.	Molecular Formula	Compound
1	20.08	1.79	232	$C_{10}H_{20}N_2O_4$	1,3-Propanediol, 2-methyl-2-(1-methylpropy l)-, dicarbamate
2	21.08	0.56	312.49	$C_{19}H_{36}O_3$	Octadecanoic acid, 9,10-epoxy methyl ester, cis-
3	23.07	0.96	338	$C_{21}H_{26}N_2O_2$	Aspidospermidine-3-carboxylic acid, 2,3-didehydro-, methyl ester, (5à,12á,19à)-
4	24.56	0.42	268	$C_{16}H_{28}O_3$	Z-(13,14-Epoxy) tetradec-11-en-1-ol Acetate
5	25.39	0.41	400	$C_{28}H_{48}O$	Cholestan-3-ol, 2-methylene-, (3á,5à)-
6	27.08	12.13	256	$C_{16}H_{32}O_2$	7 cis-vaccenic acid
7	28.57	2.83	284	$C_{18}H_{36}O_2$	Hexadecanoic acid, ethyl ester
8	30.29	25.69	282	$C_{18}H_{34}O_2$	9-Octadecenoic acid (Z)-
9	30.71	1.10	280	$C_{15}H_{20}O_5$	01297107001 TETRANEURIN - A – DIOL
10	31.41	0.55	270	$C_{17}H_{30}O_2$	Hexadecadienoic acid, methyl ester
11	31.54	2.83	282	$C_{18}H_{34}O_2$	Hexadecanoic acid
12	33.58	1.96	310	$C_{20}H_{38}O_2$	cis-11-Eicosenoic acid
13	34.50	0.49	294	$C_{19}H_{34}O_2$	Z, E,E, -1,3,12-Nonadecatriene-5,14-diol
14	35.99	2.64	330	$C_{19}H_{38}O_4$	Hexadecanoic acid, 2,3-dihydroxypropyl ester
15	36.79	5.32	338	$C_{22}H_{42}O_2$	Erucic acid
16	38.25	0.70	308	$C_{20}H_{36}O_2$	Linoleic acid ethyl ester
17	38.67	4.97	356	$C_{21}H_{40}O_4$	9-Octadecenoic acid (Z)-, 2-hydroxy-1-(hydroxymethyl)ethyl ester
18	39.61	0.75	414	$C_{29}H_{50}O$	STIGMAST-5-EN-3-OL, (3á,24S)-
19	40.21	5.48	444	$C_{30}H_{52}O_2$	9,19-Cyclolanostane-3,7-diol
20	40.30	4.19	878	$C_{57}H_{98}O_6$	Trilinolein
21	40.50	3.53	444	$C_{28}H_{44}O_4$	9-Octadecenoic acid, (2-Phenyl-1,3-Dioxolan-4-YL) methyl ester, cis-
22	40.62	4.96	620	$C_{39}H_{72}O_5$	2-Hydroxy-3-[(9E)-9-Octadecenoyloxy]Propyl (9E)-9-Octadecenoate #
23	40.82	2.28	444	$C_{30}H_{52}O_2$	Tricyclo[20.8.0.0(7,16)]triacontane, 1(22),7(16)-diepoxy-
24	41.44	6.71	354	$C_{21}H_{38}O_4$	9,12-Octadecadienoic acid (Z,Z)-, 2-hydroxy-1-(hydroxymethyl)ethyl ester
25	41.78	1.55	884	$C_{57}H_{104}O_6$	9-Octadecen+oic acid, 1,2,3-propanetriyl ester, (E,E,E)-
					94.8 %

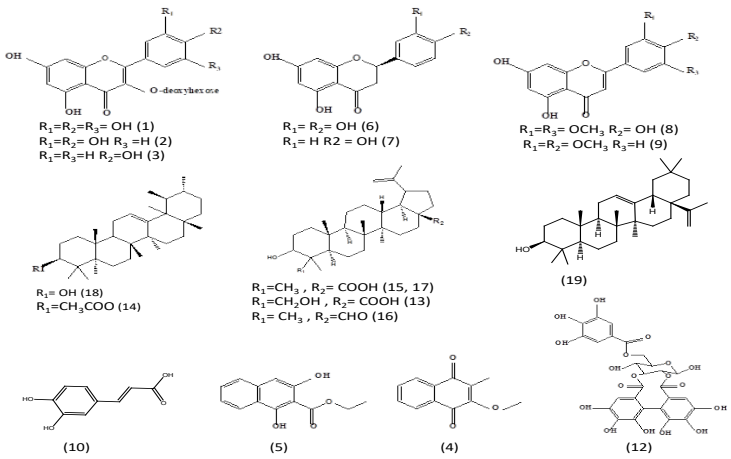

Figure 6. Fundamental structures of the tentatively identified compounds from $CHCl_3$ Fr.: (1) myricetin O-deoxyhexoside, (2) quercetin-O-deoxyhexoside, (3) kaempferol-O-deoxyhexoside (4) methoxy-methyl-1,4-naphthoquinone; (5) ethyl 1,3-dihydroxy-2-naphthoate; (6) eriodictyol; (7) naringenin; (8) tricin; (9) dihydroxy dimethoxy flavone; (10) caffeic acid; (11) oleanane-type triterpenoids; (12) hexahydroxydiphenoyl (HHDP) galloylglucose; (13) (4α)-23-hydroxy betulinic acid; (14) α-amyrin acetate; (15; 17) betulinic acid; (16) betulinaldehyde; (18) α-amyrin; (19) oleanolic acid

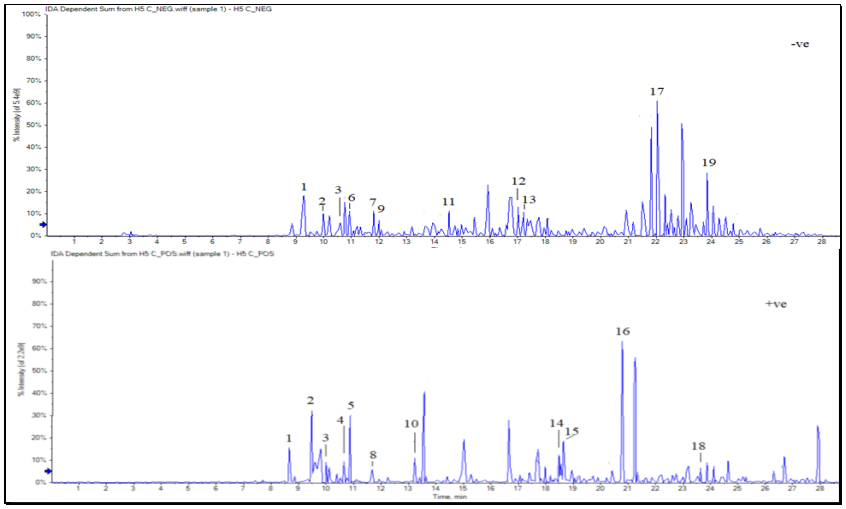

Figure 5. LC-ESI-MS –ve (a) and +ve (b) modes. of *E.r.* subsp. *schimperi* $CHCl_3$ Fraction.

Table 3. The suggested Phytochemicals in the CHCl3Fr. by LCESI-MS analysis in both negative and positive ionization modes.

NO.	RT (min)	M.F.	-ve/+ve m/z	MS/MS fragments	Tentatively compound	Referance
1	9.324 8.697	$C_{21}H_{20}O_{12}$	463 - 465 +	462.9, 316.99, 316.03, 271, 171.12, 151. 464.9, 319, 318, 273.09, 179.02, 174.7,152.09	Myricetin-O- deoxy hexoside	Nguyen et al. 2013 Pereira et al. 2017 Chaudharya et al. 2011 Abu-Reidah et al.2015
2	10.23 9.474	$C_{21}H_{20}O_{11}$	447.4 - 449 +	446,94, 301.03, 300.01, 271, 255.07, 179, 151.07. 449, 302.87, 373.75, 256.68, 153.06	Quercetin-O- deoxyhexoside	Kerebba et al. 2022 Chaudharya et al. 2011 Abu-Reidah et al.2015
3	10.022 10.638	$C_{21}H_{19}O_{10}$	431 - 433 +	285.0, 254.5, 252.8, 169.0 287.05, 257.74, 170.86	Kaempferol-O deoxyhexoside	Hassan et al 2018 Chaudharya et al. 2011 Abu-Reidah et al.2015
4	10.653	$C_{12}H_{10}O_3$	202 +	202 187, 172, 144, 142, 103, 89, 77	methoxy-methyl--1,4-naphthoquinone	Raspotnig et al. 2017
5	10.878	$C_{13}H_{12}O_4$	233 +	233, 218, 190,161	Ethyl 1,3-dihydroxy-2-naphthoate	Boritnaban et al. 2022
6	10.934	$C_{15}H_{12}O_6$	287 -	151, 135	Eriodictyol	Vijayan et al.2019
7	11.722	$C_{15}H_{12}O_5$	271 -	177, 151, 119	Naringenin	Goufo et al. 2020 Attia et al. 2022 Esteban et al., 2020
8	11.836	$C_{15}H_{10}O_5$	331 -	315, 300, 178, 153	Tricin	Li et al. 2016
9	12.009	$C_{18}H_{34}O_4$	313 -	283	dihydroxy dimethoxy flavone	Attia et al. 2022
10	13.235	$C_9H_8O_4$+	181.1 -	163, 189, 135	Caffeic acid	Avula et ai. 2022; El-Tantawy et al. 2022
11	14.547	$C_{20}H_{18}O_{14}$	469 -	469, 423, 407	oleanane type triterpenoids	Li et al. 2019
12	17.048	$C_{41}H_{28}O_{27}$	633.2 -	481, 421, 339, 301, 249	Hexahydroxydiphenoyl (HHDP) galloylglucose	El-Sayed et al. 2021
13	17.193	$C_{30}H_{46}O_3$	471 -	453, 425, 380, 203, 177	(4α)-23-hydroxy betulinic acid	Okba et al. 2021
14	18.547	$C_{32}H_{52}O_2$	468 +	468.8, 219	α-amyrin acetate	Ipav et al.,2022
15	18.680	$C_{30}H_{48}O_3$	457 +	457, 439.35, 411.36, 393.35, 189	betulinic acid	Okba et al. 2021
16	20.794	$C_{30}H_{48}O_2$	441 +	440.2891, 2.27 [M+H]+ 441, 315, 286	Betulinaldehyde	Haque et al., 2005
17	22.034	$C_{30}H_{48}O_3$	455.4 -	455.15, 407, 377, 363, 248, 207, 189.	Betulinc acid	Wu et al. 2024
18	23.644	$C_{30}H_{50}O$	426 +	219, 207, 189.	α-amyrin	Viet et al. 2021 Quintão et al, 2014
19	23.840	$C_{40}H_{58}O_5$	455.3 -	455.3, 407,391, 377, 363, 203	oleanolic acid	Chen et al. 2011 Lourenço et al. 2021

and further fragment peaks at 103 and 89, suggesting it may be methoxy-methyl-1,4-naphthoquinone (Raspotnig et al., 2017).

Compound 5: Displaying [M+H]+ ions at m/z 233, 218, 190, and 161, this compound was tentatively annotated as ethyl 1,3-dihydroxy-2-naphthoate, supported by prior research (Boritnaban et al., 2022).

Pentacyclic Triterpenes:

Compound 11: A molecular ion at m/z 469 [M-H]- showed fragment patterns at m/z 425 ([M-H]-COOH)- and 407 ([M-H]-COOH-H_2O)-, consistent with typical oleanane-type triterpene fragmentation, suggesting oleanane triterpenoids (Salih et al., 2017).

Compound 19: A single molecular ion at m/z 455.3 [M-H]- displayed fragment ions at m/z 407 [(M-H)-H_2O] and 391, 377, and 363, tentatively identified as oleanolic acid based on literature references (Chen et al., 2011). Characteristic m/z 203 peaks supported this identification, highlighting an oleanane skeleton with carboxylic or aldehyde groups (Lourenço et al., 2021).

Compound 14: Detected with a molecular ion [M+H]+ at m/z 468, along with fragments at 219 and 203, this compound was tentatively identified as α-amyrin acetate, corroborated by previous studies (Ipav et al., 2022).

Compound 18: Suggested as α-amyrin (3β-hydroxyurs-12-en-3-ol) with a [M+H]+ ion at m/z 426.3 and fragment peaks at m/z 407 [M+H-18]+ due to H_2O loss, with additional fragments at 219, 207, and 189, consistent with existing literature (Viet et al., 2021; Quintão et al., 2014).

Compound 13: Molecular ions were observed at m/z 471 [M-H]- with fragment ions at m/z 453, 425, 380, 203, and 177, indicative of hydroxy betulinic acid (Okba et al., 2021).

Compound 15: With [M+H]+ at m/z 457, fragmentation patterns at m/z 439.35 [(M+H)-H_2O]+, 411.36 [(M+H)-COOH]+, and further fragments at m/z 203.17 and 189 suggest a triterpene, potentially lupane-type triterpenes or betulinic acid aglycone (Buzgaia et al., 2021).

Compound 17: In the negative mode, this compound displayed a [M-H]- ion at m/z 455.15 with fragmentation indicating losses of formaldehyde and water, consistent with lupane-type triterpenes (Wu et al., 2024).

Compound 16: Preliminary analysis showed betulinaldehyde with a molecular ion at m/z 441.3 [M+H]+ and fragment peaks at m/z 423 [(M+H)-H_2O]+, 411 [(M+H)-HCHO]+, and 407 [(M+H)-H_2O-CH_3]+. Peaks at m/z 203, 189, and 41 [C_3H_5]+ confirm it as a lupeol-class triterpenoid, with findings consistent with existing literature on betulinaldehyde (Haque et al., 2005).

4. Discussion

These findings highlight that the chloroform fraction ($CHCl_3$ Fr.) from *E. r. ssp. shimperi* exhibits promising antidiabetic activity by inhibiting key enzymes, enhancing insulin secretion, and improving glucose regulation. Specifically, $CHCl_3$ Fr. demonstrated substantial inhibition of α-amylase and α-glucosidase enzymes, which play a central role in carbohydrate metabolism, subsequently aiding in the modulation of glucose levels and reduction of insulin resistance in IR-Huh7 cells. This fraction also reduced oxidative stress markers, including malondialdehyde (MDA) and nitric oxide (NO), though it did not exhibit significant antioxidant effects on its own. The observed effects are likely attributable to the presence of multiple bioactive compounds, particularly flavonoids, pentacyclic triterpenes, and monounsaturated fatty acids, which were identified through LC-MS/MS and GC-MS analyses.

4.1 Enzyme Inhibition:

The inhibitory action of $CHCl_3$ Fr. on α-amylase and α-glucosidase can be linked to flavonoid constituents, such as myricetin-O-rhamnoside and quercetin-O-rhamnoside (Liu et al., 2021), eriodictyol and naringenin (Li et al., 2019), and hexahydroxydiphenoyl (HHDP) galloylglucose (Lachowicz et al., 2022). These flavonoids have shown enzyme-inhibitory activity in previous studies, suggesting a synergistic effect in this extract. Additionally, pentacyclic triterpenes, including oleanolic acid and betulinic acid (Ali et al., 2022), as well as caffeic acid (Oboh et al., 2021), further contributed to enzyme inhibition, highlighting a complex interaction of multiple compounds in reducing glucose levels.

4.2 Fatty Acids and Glucose Regulation:

The presence of 9-octadecenoic acid (Z), a predominant monounsaturated fatty acid identified in GC-MS of $CHCl_3$ Fr., also supported enzyme inhibition, as suggested by previous studies (Yang et al., 2017). Additionally, oleanolic and betulinic acids, along with α-amyrin, were found in the LC-MS/MS profile of $CHCl_3$ Fr. These compounds have shown the potential to improve insulin sensitivity and reduce hepatic glucose levels, possibly contributing to their antidiabetic effects by reducing oxidative stress in diabetic models (Fernández-Aparicio et al., 2022; Birgani et al., 2018; Ajala-Lawal et al., 2014; Santos et al., 2012). Moreover, oleic acid (9-octadecenoic acid, omega-9), which constituted 25.69% of the extract, has been shown to reduce insulin resistance by regulating PI3K signaling pathway genes (López-Gómez et al., 2021). Similarly, cis-vaccenic acid (omega–7) at 12.13% content was also linked to decreased insulin resistance and a reduced risk of diabetes (Weir et al., 2012; Abbirami et al., 2019).

4.3 Antioxidant Properties: Flavonoids, such as myricetin-3-O-rhamnoside and quercetin-3-O-rhamnoside previously isolated from this plant, exhibited radical scavenging activities (Liu et al., 1997), which have been shown to reduce MDA levels and prevent oxidative stress in diabetic conditions (Mihailović, 2021). Tricin, another flavonoid in the fraction, could block MDA production, further preventing oxidative damage (Yang & Li, 2023). The

hydroxyl group quantity and positioning within flavonoid structures also play a pivotal role in modulating their antioxidant properties (Shamsudin et al., 2022).

4.4 Role of Triterpenoids in Insulin Sensitivity and Organ Protection:

The pentacyclic triterpenoids, particularly those with C-3 substitutions, enhance antidiabetic efficacy, as shown in past studies (Banerjee et al., 2019; Oršolić et al., 2021). Treatment with caffeic acid demonstrated a protective effect on both kidney and liver functions in diabetic conditions, likely due to its regulatory effects on glucose metabolism and reduction of oxidative stress (Oboh et al., 2021). These insights indicate that pentacyclic triterpenes and their derivatives significantly contribute to the multifaceted antidiabetic actions of $CHCl_3$ Fr. In summary, the diverse classes of bioactive compounds present in $CHCl_3$ Fr., such as flavonoids, unsaturated fatty acids, and pentacyclic triterpenes, collectively contribute to its ability to treat diabetes and mitigate associated complications. This multipronged approach suggests that $CHCl_3$ Fr. could serve as a therapeutic option for managing glucose metabolism, reducing oxidative stress, and improving insulin sensitivity (Banerjee et al., 2019; Nazaruk et al., 2021; Mirmiran et al., 2018).

5. Conclusion

the chloroform fraction ($CHCl_3$ Fr.) from *E. r. ssp. shimperi* demonstrates significant potential as a therapeutic agent for diabetes management. This extract exhibits a broad spectrum of bioactivities, notably inhibiting α-amylase and α-glucosidase enzymes, enhancing insulin secretion, and modulating glucose regulation, all of which contribute to reduced insulin resistance and improved glucose metabolism. Key bioactive compounds identified, including flavonoids (such as myricetin-O-rhamnoside and quercetin-O-rhamnoside), pentacyclic triterpenes (including oleanolic acid and betulinic acid), and monounsaturated fatty acids like 9-octadecenoic acid, play central roles in these effects by promoting insulin sensitivity, regulating key metabolic pathways, and mitigating oxidative stress. These findings support the therapeutic potential of $CHCl_3$ Fr. in diabetes management, highlighting the synergistic interactions among its various bioactive compounds as valuable contributors to its antidiabetic and antioxidative properties. Further studies could deepen understanding and enhance its clinical applicability.

Author contributions

H.M.E. was responsible for the conceptualization, design, and drafting of the manuscript. The author reviewed and approved the final version of the manuscript.

Acknowledgment

The authors were grateful to their department.

Competing financial interests

The authors have no conflict of interest.

References

Abbirami, E.L., Kumar, D., Guna, R., Gayathr, N., Sivasudh, T. (2019). Alpha Amylase, Alpha Glucosidase Inhibition and Profiling of Volatile Compounds of Biologically Active Extracts from Momordica cymbalaria (Hook, Fenzl) Skin and Seeds, Asia Pac J Sci Technol 8(1): 67-73© https://doi.org/10.51983/ajeat-2019.8.1.1057.

Abd El-Kareem, M.S., Rabbih, M.A.E.F., Selim, E.T.M., Elsherbiny, E,A,E,M., El-Khateeb, A.Y. (2016). Application of GC/EIMS in combination with semi-empirical calculations for identification and investigation of some volatile components in basil essential oil. Int'l J. of Analytical Mass Spectrometry and Chromatography 4(1): 14-25. http://dx.doi.org/10.4236/ijamsc.2016.41002.

Abu-Reidah, I.M., Ali-Shtayeh, M.S., Jamous, R.M., Arráez-Román, D., Segura-Carretero, A. (2015). HPLC–DAD–ESI-MS/MS screening of bioactive components from Rhus coriaria L. (Sumac) fruits. Food Chem 166:179-191. https://doi: 10.1016/j.foodchem.2014.06.011.

Agus, S., Achmadi, S.S., Mubarik, N.R. (2017). Antibacterial activity of naringenin-rich fraction of pigeon pea leaves toward Salmonella thypi. Asian Pac J Trop Biomed 7(8): 725-728. https://doi. org/10.1016/j.apjtb.2017.07.019.

Ajala-Lawal, R.A., Aliyu, N.O., Ajiboye, T.O., (2020). Betulinic acid improves insulin sensitivity, elevated blood glucose, antioxidants, inflammation and dyslipidaemia and oxidative stress. Arch Physiol Biochem 126(2):107-115. https://doi.org/10.1080/1381-3455. 2018.1498901.

Ali, M.S., Jahangir, M., Hussan, S.S., Choudhary, M.I. (2002). Inhibition of α-glucosidase by oleanolic acid and its synthetic derivatives. Phytochem60:295–299. https://doi: 10.1016-/s00319422(02)-00104-8.

Asres, K., Gibbons, S., Bucar, F. (2006). Radical scavenging compounds from ethiopian medicinal plants. Ethiop Pharm J 24 (1): 23-30. https://doi:10.4314/epj.v24i1.-35095.

Attia, R,A., El-Dahmy, S.I., Abouelenein, D.D., Abdel-Ghani, A.E. (2022). LC-ESI-MS profile, cytotoxic, antioxidant, insecticidal and antimicrobial activities of wild and in vitro propagated Tanacetum sinaicum Del. ex DC. Zagazig J. Pharm. Sci. 31(2): 8- 21. https:// doi. 10.21608/ZJPS.2022.-157581.1041.

Avula, B., Sagi, S., Masoodi, M.H., Ji-Yeong, B., Wali, A.F., Khan, I.A. (2020). Quantification and characterization of phenolic compounds from Northern Indian Propolis extracts and dietary supplements. J AOAC Int 103(5): 1378–1393. https://doi.org/10.1093/jaoacint-/qsaa-032.

Banerjee, S., Bose, S., Mandal, M.S.C., Dawn, S.M., Sahoo, U., Ramadan. M.A., Mandal, S.K. (2019). Pharmacological property of pentacyclic triterpenoids. Egypt J Chem 62(1): 13 – 35. https://doi.org/10.21608/ejchem.-2019.16055.1975.

Birgani, G.A., Ahangarpour, A., Khorsandi, L., Moghaddam, H.F. (2018). Anti-diabetic effect of betulinic acid on streptozotocin-nicotinamide induced diabetic male mouse model. Braz J Pharm Sci 54 (2): e17171- 7. https://doi.org/10.1590/s217597902018-000217171.

Boritnaban, D.A., Karomah, A.H., Septaningsih, D.A., Majiidu, M., Dwiyanti, F.G., Siregar, I.Z., Rafi, M. (2022). Metabolite Profiling of Ebony (Diospyros celebica Bakh) leaves and wood extracts using LC-MS/MS. Indones J Chem 22 (2): 352 – 360. http://dx.doiorg/10.22146/ijc.-68529.

Botha, E. (2016). "Investigating the production of secondary metabolites effective in lowering blood glucose levels in Euclea undulata Thunb. Var Myrtina (Ebenaceae)". Env Sci., p 120. https://api.semanticscholar-.org/Corpus-ID:99557343.

Buzgaia, N., Soo. Y.L., Rukayadi, Y., Abas. F., Shaari. K. (2021). Antioxidant Activity, α-Glucosidase Inhibition and UHPLC–ESI–MS/MS Profile of Shmar (Arbutus pavarii Pamp). Plants (Basel) 10(8): 1659. https://doi: 10.3390/plants10081659.

Chaudharya, A., Kaura, P., Kumara, N., Singha, B., Awasthia, S., Lalb, B. (2011). Chemical fingerprint analysis of phenolics of Albizia chinensis based on ultra-performance LC-electrospray ionization-quadrupole time-of-flight mass spectrometry and antioxidant activity. Nat Prod Commun 6 (11): 1617 – 1620. https://doi:10.1177/1934578x-110060-1115.

Chen, Q., Zhang, Y., Zhang, W., Chen, Z. (2011). Identification and quantification of oleanolic acid and ursolic acid in Chinese herbs by liquid chromatography–ion trap mass spectrometry. Biomed Chromatogr 25 (12): 1381–1388. https://doi: 10.1002/bmc.1614.

Draper, M.H.H., Hadley, M. (1990). Malondialdehyde determination as index of lipid peroxidation. Methods Enzymol. 186:421-31. https://doi: 10.1016/0076-6879(90)86135-i.

El-Sayed, M.A., Abbas, F,A., Refaat, S., El-Shafae, A.M., Fikry, E. (2021). UPLC-ESI-MS/MS profile of the ethyl acetate fraction of aerial parts of Bougainvillea 'Scarlett O'Hara' cultivated in egypt. Front Ecol Evol 64 (2): 793 – 806. https://doi.10.21608-/EJCHEM.2020.45694.2933.

El-Tantawy. H.M., Hassan. A.R., Taha. H.E. (2022). Anticancer mechanism of the non-polar extract from Echium angustifolium Mill. aerial parts in relation to its chemical content. Egypt J Chem 65 (10):17-26. https://doi.10.21608/EJCHEM.2022.130795.5757.

Esteban, M.A., Sánchez-Hernández, S., Samaniego, S.C., Olalla, H.M. (2020). Differences in the phenolic profile by UPLC coupled to high resolution mass spectrometry and antioxidant capacity of two Diospyros kaki varieties. Antioxidants (Basel) 10(1): 31-40. https://-doi: 10.3390/antiox10010031.

Fernández-Aparicio, Á., Correa-Rodríguez, M., Castellano, J.M., Valle, J.S.R., González-Jiménez, E. (2022). Potential Molecular Targets of Oleanolic Acid in Insulin Resistance and Underlying Oxidative Stress: A Systematic Review. Antioxidants (Basel), 11(8): 1517. https://doi.org/10.3390/-antiox11081517.

Gaweł, S., Wardas, M., Niedworok, E., Wardas, P. (2004). Malondialdehyde (MDA) as a lipid peroxidation marker. Wiad Lek 57 (9-10): 453-5. PMID: 15765761.

Gong, L., Feng, D. Wang, T. Ren, Y., Liu, Y., Wang, J. (2020). Inhibitors of α-amylase and α-glucosidase: Potential linkage for whole cereal foods on prevention of hyperglycemia. Food Sci Nutr 8(12): 6320–6337. https://doi.org/10.1002/fsn3.1987.

Goufo, P., Singh, R.K., Cortez, I. (2020), A reference list of phenolic compounds (including stilbenes) in grapevine (Vitis vinifera L.) roots, woods, canes, stems, and leaves. Antioxidants (Basel). 9(5): 398- 435. https://doi: 10.3390/antiox9050398.

Grover, J.K., Yada,. S. Vats, V. (2002). Medicinal plants of India with anti-diabetic potential. J. Ethnopharmacol 81(1):81–100. https:// doi: 10.1016/s0378-8741(02)00059-4.

Haque. MdE., Shekhar. H.U., Mohamad. A.U., Rahman. H., Mydul. I.A.M., Hossain. M.S. (2005). Triterpenoids from the stem bark of Avicennia officinalis. . Pharm Sci 5(1-2):53-57. https://doi:10.3329/dujps.v5i1.229.

Hassan, A.R. (2022). Chemical profile and cytotoxic activity of a polyphenolic-rich fraction from Euphorbia dendroides aerial parts. S Afr J Bot. 147, 332-339. https://doi.org/10.-1016/j.-sajb.2022.01.035.

Hassan, W.H.B., Abdel-aziz, S., Al Yousef, H.M. (2018). Chemical composition and biological activities of the aqueous fraction of Parkinsonea aculeata L. growing in saudi arabia. Arab J Chem 12(3):377-387. https://doi.org/10.1016/j.arabjc.2018.08.003.

Ipav, S.S., Igoli, J.O., Tor-Anyiin, T.A. (2022). Isolation and characterization of alpha and beta amyrins from Propolis obtained from benue state. J Chem Soc Nigeria 47(2): 250 –261. https://doi.org/10.46602/jcsn.v47i2.723.

Jakovljevic, N.K. Pavlovic, K. Zujovic, T, Kravic-Stevovic, T. Jotic, A. Markovic, I. Lalic, N.M. (2021). In vitro models of insulin resistance: Mitochondrial coupling is differently affected in liver and muscle cells. Mitochondrion 61: 165-173. https://doi: 10.1016/j.mito.-2021.10.001.

Kerebba, N., Oyedeji, A.O., Byamukama, R., Kuria, S.K., Oyedeji, O.O. (2022). UHPLC-UHPLC-ESI-QTOF-MS/MS characterisation of phenolic compounds from Tithonia diversifolia (Hemsl.) A. Gray and Antioxidant Activity. ChemistrySelect 7(16): e202104406-22. https://doi.org/10.1002/slct.202104406.

Lachowicz, S., Oszmianski, J., Rapak, A., Ochmian, I.M. (2020). Profile and content of phenolic compounds in leaves, flowers, roots, and stalks of Sanguisorba officinalis L. determined with the LC-DAD-ESI-QTOF-MS/MS analysis and their in vitro antioxidant, antidiabetic, antiproliferative potency. J Pharm 13(8): 191-214. https://doi: 10.3390/ph-13080191.

Leighton, E., Sainsbury, C.A., Jones, G.C. (2017). A Practical review of C-Peptide testing in diabetes. Diabetes Ther 8(3):475-487. https://doi: 10.1007/s13300-017-0265-4.

Li, M., Pu, Y., Yoo, C.G., Ragauskas, A.J. (2016). The occurrence of tricin and its derivatives in plants. Green Chem18(6):1439-1454. . DOI: 10.1039/x0xx00000x

Li. S., Zhang, Y., Sun, Y., Zhang, G., Bai, J., Guo. J., Su, X., Du, H., Cao, X., Yang, J., Wang, T. (2019). Naringenin improves insulin sensitivity in gestational diabetes mellitus mice through AMPK. Nutr Diabetes. 9 (28): 10. https://doi: 10.1038/s41387-019-0095-8

Liu, Y., Peterson, D.A., Kimura, H., Schubert, D. (1997). Mechanism of cellular 3-(4,5-dimethylthiazol-2-yl)-2,5-diphenyltetrazolium bromide (MTT) reduction. J Neurochem 69(2):581-93. https://doi: 10.1046/j.1471-4159.1997.69020581.x.

Liu. X., Fu. Y., Ma. Q., Yi., J., Cai. S., (2021). Anti-diabetic effects of different phenolic-rich fractions from Rhus chinensis Mill. fruits in vitro. eFood. (1):37–46. https:// doi:10.2991-/efood-.k.210222.002.

López-Gómez, C., Santiago-Fernández, C., García, S., García-Escobar, E. Gutiérrez-Repiso, C. Rodríguez-Díaz, C, Ho-Plágaro, A. Martín-Reyes, F. Garrido-Sánchez, L., Valdés, S., Rodríguez-Cañete, A., Rodríguez-Pacheco, F., García-Fuentes, E. (2021).

Oleic acid protects against insulin resistance by regulating the genes related to the PI3K signaling pathway. J Clin Med9(8): 2615- 2629. https://doi.org/10.3390/jcm9082615.

Lourenço, A., Marques, A.V., Gominho, J. (2021). The identification of new triterpenoids in Eucalyptus globulus wood. Mol 26(12): 3495.-3508. https://doi.org/10.3390%-Fmolecules-26123495.

Mechchate, H., Es-safi, I., Louba, A., Alqahtani, A.S., Nasr, F.A. Noman, O,M., Farooqm M., Alharbi, M.S., Aziz, A., Bari, A., Hicham, B., Bousta, D. (2021). In vitro alpha-amylase and alpha-glucosidase inhibitory activity and in vivo antidiabetic activity of Withania frutescens L. foliar Extract. Mol 26 (2): 293 https://doi.org/10.3390/molecules-26020293.

Mekonnen, A., Atlabachew, M. Kassie, B. (2018). Investigation of antioxidant and antimicrobial activities of Euclea schimperi leaf extracts. Chem biol technol Agric 5): 16(https://doi. org/10.-1186/s40538-018-0128-x

Mihailović, M., Dinić, S., Jovanović, J.A., Uskoković, A., Grdović, N., Vidaković, M. (2021). The influence of plant extracts and phytoconstituents on antioxidant enzymes activity and gene expression in the prevention and treatment of impaired glucose homeostasis and diabetes complications. Antioxidants (Basel) 10(3): 480-505. https://doi.org/10.3390/antiox-10030480.

Mirmiran, P., Esfandyari, S., Moghadam, S.K., Bahadoran, Z., Azizi, F. (2018). Fatty acid quality and quantity of diet and risk of type 2 diabetes in adults:Tehran Lipid and Glucose Study. J Diabetes Complications 32(7): 655–659. https://doi.org/10.1016/j.jdiacomp.2018.-05.003.

Mishra, S., Mishra, B.B. (2017) Study of lipid peroxidation, nitric oxide end product, and trace element status in type 2 diabetes mellitus with and without complications. Int J Appl Basic Med Res 7(2): 88–93. https://doi: 10.4103/2229-516X.205813

Nazaruk, J., Kluczyk, B.M. (2015). The role of triterpenes in the management of diabetes mellitus and its complications. Phytochem Rev 14(4): 675–690. https://doi.org/10.1007/-s111-01-014-9369-x.

Nguyen, H.T., Pandey, R.P., Thuy, T.T.T, Park, J,W., Sohng, J.K, (2013). Improvement of Regio-Specific Production of Myricetin-3-O-α-L-Rhamnoside in Engineered Escherichia coli. Appl Biochem Biotechnol 171(8): 1956–1967. https:// doi 10.1007/s12010-013-0459-9

Oboh, M., Govender, L., Siwela, M., Mkhwanazi, B.N., (2021). Anti-diabetic potential of plant-based pentacyclic triterpene derivatives: progress made to improve efficacy and bioavailability. Mol 26(23): 7243-7264. https://doi.org/10.3390%2Fmolecules-26237243.

Odukoya, J.O., Odukoya, J.O., Mmutlane, E.M., Ndinteh, D.T.)2022(. Ethnopharmacological Study of Medicinal Plants Used for the Treatment of Cardiovascular Diseases and Their Associated Risk Factors in sub-Saharan Africa. Plants (Basel) 11 (10): 1387. doi: 10.3390/plants-11101387

Okba, M.M., El-Shiekh, R.A., Abu-Elghait, M., Sobeh, M., Ashour. R.M.S. (2021). HPLC-PDA-ESI-MS/MS profiling and anti-Biofilm potential of Eucalyptus sideroxylon Flowers. Antibiot 10(7):761-778. https://doi: 10.3390/antibiotics10070761.

Ormazabal, V., Soumyalekshmi, N. Elfeky, O., Aguayo, C. Salomon, C., Zuñiga, F.A. (2018). Association between insulin resistance and the development of cardiovascular disease. Cardiovasc Diabetol 17:122 https://doi.org/-10.1186/s12933-018-0762-4

Oršolić, N., Damir, S., Odeh. D., Gajski, G., Balta, V., Šver, L., Jembrek, M.J. (2021). Efficacy of Caffeic Acid on Diabetes and Its Complications in the Mouse. Mol 26 (11): 3262. https://doi.org/10.3390/molecules26113262.

Pereira, P., Cebola, M., Oliveira, M.C., Gil, G.B.M. (2017). Antioxidant capacity and identification of bioactive compounds of Myrtus communis L. extract obtained by ultrasound-assisted extraction. J Food Sci Technol. 54(13):4362-4369. https://doi: 10.1007/s13197-017-2907-y. 1

Prieto, P., Pineda, M. Aguilar, M. (1999). Spectrophotometric quantitation of antioxidant capacity through the formation of a phosphomolybdenum complex: Specific application to the determination of vitamin E. Anal Biochem 269 (2):337-41. https://doi.org/10.1006/-abio.1999.4019

Quintão, N.L.M., Rocha, W., Silva, G.F., Reichert, S., Claudino, V.D., Lucinda-Silva. R.M., Malheiros, A., De Souza, M.M., Filho, V.C., Bresolin, T.M.B., Machado, M.d.S., Wagner, T.M., Meyre, S.C. (2014). Contribution of α,β-amyrenone to the anti-inflammatory and antihypersensitivity effects of Aleurites moluccana (L.) willd. Biomed Res Int 636839-50. https://doi: 10.1155-/2014/636839.

Raspotnig, G., Schaider, M., Föttinger, P., Schönhofer, A. (2017). A model for phylogenetic chemosystematics: Evolutionary history of quinones in the Scent Gland secretions of Harvestmen. Nat Ecol Evol 17(5): 139. https://doi.org-/10.3389%2Ffevo.2017-.00139.

Rigler, R., Pramanik, A., Jonasson, P., Kratz, G., Jansson, O.T., Nygren, P., Ståh, S., Ekberg, K., Johansson, B., Uhlén, S., Uhlén, M., Jörnvall, H. Wahren, J. (1999). Specific binding of proinsulin C-peptide to human cell membranes. Proc Natl Acad Sci USA 96(23):13318-23. https://doi: 10.1073/pnas.96.23.13318.

Salih, E.Y.A., Fyhrquist, P., Abdalla, A.M.A., Abdelgadir, A.Y., Kanninen, M., Sipi, M., Luukkanen, O., Fahmi, M.K.M., Elamin, M.H., Ali, H.A. (2017). LC-MS/MS Tandem mass spectrometry for analysis of 3 Phenolic compounds and pentacyclic triterpenes in antifungal extracts of Terminalia brownii (Fresen). Antibiotics 6 (4):37-59. https://doi.org/10.3390%2-Fantibiotics-6040037.

Santos, F.A., Frota, J.T., Arrud, B.R., de Melo, T.S., da Silva, A.C.A., Brito, G.A.C., Chaves, M.H., Rao, V.S. (2012). Antihyperglycemic and hypolipidemic effects of α, β-amyrin, a triterpenoid mixture from Protium heptaphyllum in mice. Lipids Health Dis11: (98): 1476-511. https://doi.org/10.1186/1476-511X-11-98.

Shai LJ, Magano SR, Lebelo SL, Mogale AM (2011) Inhibitory effects of five medicinal plants on rat alpha-glucosidase: Comparison with their effects on yeast alpha-glucosidase. J Med Plant Res 5(13):2863-2867. http://www.academicjournals.org/-JMPR.

Shamsudin, N.F., Ahmed, Q.U., Mahmood, S., Shah, S.A.A., Sarian, M.N., Khattak, M. A.K., Khatib, A., Sabere, A.S.M, Yusoff, Y.M.D., Latip, J. (2022). Flavonoids as antidiabetic and anti-Inflammatory agents: A review on structural activity relationship-based studies and meta-analysis. Int J Mol Sci 23(20): 12605. https://doi.org/10.3390-/ijms232012605.

Spínola, V., Pinto, J., Castilho, P.C, (2015). Identification and quantification of phenolic compounds of selected fruits from Madeira Island by HPLC-DAD–ESI-MSn and screening for their antioxidant activity. Food Chem 173:(14-30). https://doi: 10.1016/j.food-chem. 2014.09.163.

Steiner, D.F., Cunningham, D., Spigelm, L., Aten, B. (1967). Insulin biosynthesis: evidence for a precursor. Sci 157(3789):697-700. https://doi: 10.1126/science.157.3789.697.

Tamil, I.G., Dineshkumar, B., Nandhakumar, M., Senthilkumar. M., Mitral, A. (2010). In vitro study on α-amylase inhibitory activity of an Indian medicinal plant. J Pharmacol 42(5): 280–282. https:// doi: 10.4103/0253-7613.70107.

Taye, A.D., Bizuneh, G.K. Kasahun, A.E. (2023). Ethnobotanical uses, phytochemistry and biological activity of the genus Euclea: A review. Front pharmacol 14: 1170145. doi: 10.3389/-fphar.2023.1170145. 62.

Telagari, M., Hullatti, K. (2015). In-vitro α-amylase and α-glucosidase inhibitory activity of Adiantum caudatum Linn. and Celosia argentea Linn. extracts and fractions., Indian J Pharmacol 47(4): 425–429. https://doi:10.4103/0253-7613.161270.

Torun, A.N., Kulaksizoglu. S., Kulaksizoglu, M., Pamuk, B.O., Isbilen, E., Tutuncu, N.B. (2009). Serum total antioxidant status and lipid peroxidation marker malondialdehyde levels in overt and subclinical hypothyroidism J Clin Endocr70(3):469-74. https://doi.org/-10.1111/j.1365-2265.2008.03348.x

Tundis, R., Loizzo, M.R., Menichini, F. (2010). Natural products as alpha-amylase and alpha-glucosidase inhibitors and their hypoglycaemic potential in the treatment of diabetes: an update. Mini Rev Med Chem 10(4):315-31. https://doi: 10.2174/13895571079133-1007.

Viet, T.D., Xuan. T.D., Anh, L.H. (2021). α-Amyrin and β-Amyrin isolated from Celastrus hindsii leaves and their antioxidant, anti-xanthine oxidase, and anti-tyrosinase potentials. Mol 26(23): 7248-7262. https://doi: 10.3390/molecules26237248.

Vijayan, K.P.R., Raghu, A.V. (2019). Tentative characterization of phenolic compounds in three species of the genus Embelia by liquid chromatography coupled with mass spectrometry analysis. An Macromol Rapid Commun 52(10): 1532-2289. https://doi.org/10.1080/-00387010.2019-.1682013.

Villalva-Pérez, J.M., Ramírez-Vargas, M.A., Serafín-Fabían, J.I., Ramírez, M., Moreno-Godínez, M.E., Espinoza-Rojo, M. Flores-Alfaro, E. (2020). Characterization of Huh7 cells after the induction of insulin resistance and post-treatment with metformin. Cytotechnology 72(4): 499–511. https://doi: 10.1007/s10616-020-00398-4.

Weir, N.I., Johnson, L., Guan, W., Steffen, B., Djousse, L., Mukamal, K.J., Tsai, M.Y, Woźniak, A., Paduch, R. (2012). Aloe vera extract activity on human corneal cells. Pharm Biol. 2012; 50(2): 147–154. https://doi.org/3A10.3109-/13880209.2011.579980

Woźniak, A., Paduch, R. (2012). Aloe vera extract activity on human corneal cells. Pharm Biol. 50(2): 147–154. http:// doi: 10.3109/13880209.2011.579980.

Wu. J., Wang. Z, Cheng. X., Lian. Y., An. X., Wu. D. (2024). Preliminary study on total component analysis and in vitro antitumor activity of Eucalyptus leaf residues. Mol 29(2): 280-298. https://doi: 10.3390-/molecules29020280.

Wube, A.A., Streit, B., Gibbons, S., Asres, K., Bucara., F. (2005). In vitro 12(S)-HETE inhibitory activities of naphthoquinones isolated from the root bark of Euclea racemosa ssp. Schimperi. J Ethnopharmacol 102(2): 191-196. https:// doi: 10.1016/j.jep.2005.06.009.

Yang, H., Jin, X., Lam, C.W., Yan, S.K. (2011). Oxidative stress and diabetes mellitus. Clin Chem Lab Med 49 (11):1773-82. https://doi: 10.1515/CCLM-.2011.250.

Yang, J.Y., Park, J.H., Chung, N., Lee, H.S. (2017). Inhibitory Potential of Constituents from Osmanthus fragrans and Structural Analogues Against Advanced Glycation End Products, α-Amylase, α-Glucosidase, and Oxidative Stress. Sci Rep 7:45746. https://doi: 10.1038/srep45746.

Yang, X., Li, D. (2023). Tricin attenuates diabetic retinopathy by inhibiting oxidative stress and angiogenesis through regulating sestrin 2/Nrf2 signaling. Hum Exp Toxicol 42: 1-10. https://doi.org/10.1177/09603271231171642.